STUDIES

A modified spatial cross-correlation measure for time-dependent spatial panel data

Rahma Fitriani
(corresponding author)
Department of Statistics,
University of Brawijaya,
Malang, Indonesia
Email: rahmafitriani@ub.ac.id

Eni Sumarminingsih
Department of Statistics,
University of Brawijaya,
Malang, Indonesia

Luthfatul Amaliana
Department of Statistics,
University of Brawijaya,
Malang, Indonesia

Nisa Dwirahma Widhiasih
Department of Statistics,
University of Brawijaya,
Malang, Indonesia

A spatial cross-correlation is a measure of the interaction of one local variable on another variable of the surrounding regions. In regional economics, the observed variables are mostly dynamic over time. When the time dimension is accommodated using spatial panel data, the time dependence can be addressed properly. Therefore, this study aims to formulate a dynamic time-dependent spatial cross-correlation index based on spatial panel data. The conducted simulation study shows the good performance of the measure. It also performs well in measuring the spatial cross-correlation between regional GDP growth and the percentage of urban population of the 38 East Java regencies/municipalities.

Introduction

In the context of regional economic analysis, spatial data are a set of observed values of geographically referenced regional economic indicators (e.g., economic growth, population density). The indicators commonly have spatial interaction, which is measured by spatial correlation. Statistically, the degree of relationship between an observed variable in a region and observations of the same variable in its surrounding regions is defined as spatial autocorrelation. Several indices, such as Moran's I and Geary's C, are used to measure spatial autocorrelation (Anselin 2017, Duran–Karahasan 2022). In the modelling process, the significance of the spatial autocorrelation indicates the need to accommodate a spatial lag of the dependent variable in the model.

On the other hand, Chen (2015) defines the relationship degree between an observed variable (X) in a region and observations of another variable (Y) in its surrounding regions as a spatial cross-correlation. The significance of the spatial cross-correlation indicates a strong relationship between the local value of X and the neighbourhood values of Y or vice versa. When it is plausible to assume a causal relationship, this situation leads to the choice of a model with a spatial lag of the independent variable.

The concept of spatial cross-correlation has been mentioned in several studies (Cheng et al. 2020, Duffy–Hughes-Clarke 2005, Loth–Baker 2013, Lamb et al. 2014). These studies are mainly in the field of geospatial science. In Loth–Baker (2013) and Cheng et al. (2020), spatial cross-correlation is used to measure the degree of similarity between certain characteristics observed in two locations that are h unit distances apart at two different points in time. The first study focuses more on the measure, whereas the latter uses the measure to model the spectral elastic input energy of ground motions. In addition to measuring the degree of similarity, Duffy–Hughes-Clarke (2005) apply the spatial cross-correlation technique to determine two locations with similar spatial datasets.

A correlation between two time series is known as a cross-correlation. In Arianos–Carbone (2009), it is defined as a function of time lag τ. Therefore, the cross-correlation measures the correlation between $X(t)$ and $Y(t + \tau)$. The concept that is used in Chen (2015), as well as in this study, is analogous to the time series cross-correlation measure. Specifically, when it is applied for two distinct spatial variables, the time index is substituted by the location index, and the time lag is replaced by the spatial lag. However, Chen's (2015) spatial cross-correlation index is calculated based on a set of spatial data observed at one time period. Since the spatial interaction of several regional economic indicators exhibits a time dynamic interdependence, the index must accommodate the time dynamic and be calculated based on a set of spatial panel data.

Several studies (Henderson 2003, Abdel-Rahman et al. 2006, Hong et al. 2021, Liddle–Messinis 2013) have addressed the potential correlation between economic

growth and urbanization indicators (e.g., degree of urban concentration, urban population, or urban primacy) in the absence of spatial and time dependence. Chen et al. (2014) note the similar spatial pattern of regional expansion and economic growth, which indicates the spatial interaction between regions in terms of those two variables. When a set of panel data is used, Abdel-Rahman et al. (2006) or Henderson (2003) show the dynamic relation between those two variables. Therefore, with the construction of this new index, using a set of spatial panel data, time-dependent spatial cross-correlation between economic growth and urbanization can be measured.

The objective of this study is to develop a time-dependent spatial cross-correlation index to measure the time-dependent spatial interaction between two sets of spatial panel data. A simulation study is conducted to analyse the performance of the developed index. The index is then used to study the nature of the time-dependent spatial interaction between regional GDP growth and the percentage of the urban population of 38 East Java regencies/municipalities during 2014–2019. The result provides a different insight into the interaction between economic growth and urbanization, which can be applied to another region with similar characteristics.

Materials and methods

This section begins with an explanation of the proposed index, a description of the data and the study area, and the setting of the simulation study.

Spatial cross-correlation index for time-dependent spatial panel data

In this study, several modifications of Chen's (2015) spatial cross-correlation index are made to adjust for the spatial panel data setting. The index was originally developed for a set of spatial data.

The first modification is for the data vector. Two vectors representing the spatial panel data for variables X and Y observed in each of N spatial units during T time periods are defined as:

$$\boldsymbol{X} = [X_{11} \quad \ldots \quad X_{N1} \quad \ldots \quad X_{1T} \quad \ldots \quad X_{NT}]^T \tag{1}$$

$$\boldsymbol{Y} = [Y_{11} \quad \ldots \quad Y_{N1} \quad \ldots \quad Y_{1T} \quad \ldots \quad Y_{NT}]^T \tag{2}$$

respectively. Following the definition in Chen (2015), the standardized vectors are used to maintain the property of correlation index value (between –1 to 1). The standardized panel data vectors are defined here as:

$$\boldsymbol{x} = [x_{11} \quad \ldots \quad x_{N1} \quad \ldots \quad x_{1T} \quad \ldots \quad x_{NT}]^T \tag{3}$$

$$\boldsymbol{y} = [y_{11} \quad \ldots \quad y_{N1} \quad \ldots \quad y_{1T} \quad \ldots \quad y_{NT}]^T \tag{4}$$

in which the elements of each vector are:

$$x_{it} = \frac{X_{it} - \bar{X}_{.t}}{S_{.t}^X} \tag{5}$$

$$y_{it} = \frac{Y_{it} - \bar{Y}_{.t}}{S_{.t}^Y} \tag{6}$$
$$i = 1, \dots, N, t = 1, \dots, T$$

In   (5) and (6), the average over all spatial units is obtained for each period, $t = 1,\dots,T$, according to the following definitions:

$$\bar{X}_{.t} = \frac{1}{N} \sum_{i=1}^{N} X_{it} \tag{7}$$

$$\bar{Y}_{.t} = \frac{1}{N} \sum_{i=1}^{N} Y_{it} \tag{8}$$

for variables X and Y, respectively. In   (5) and (6), the standard deviation over all spatial units is also obtained for each period, $t = 1,\dots,T$, according to the following definitions:

$$S_{.t}^X = \sqrt{\frac{1}{N-1} \sum_{i=1}^{N} (X_{it} - \bar{X}_{.t})^2} \tag{9}$$

$$S_{.t}^Y = \sqrt{\frac{1}{N-1} \sum_{i=1}^{N} (Y_{it} - \bar{Y}_{.t})^2} \tag{10}$$

for variables X and Y, respectively. It can be shown that:
$$\|\boldsymbol{x}\| = \boldsymbol{x}^T \boldsymbol{x} = T(N-1) \tag{11}$$
and

$$\|\boldsymbol{y}\| = \boldsymbol{y}^T \boldsymbol{y} = T(N-1) \tag{12}$$

The second modification is for the spatial weight matrix. This study uses the space time weight matrix, which is similar to the one defined in Wang–Lam (2020) and Fitriani et al. (2022). The weight is defined by assuming that a variable observed in location $i, i = 1, \dots, N$ at time $t, (X_{it})$ depends on another variable observed at the neighbouring locations at the same time $(Y_{jt}, j \neq i, j \in \text{Neighbouring of } i, i = 1, \dots, N)$ and the neighbouring locations observed at t', previous or future period $(Y_{jt'}, j \neq i, j \in \text{Neighbouring of } i, i = 1, \dots, N)$.

The space-time weight matrix is defined as:
$$\boldsymbol{V} = \boldsymbol{W}_T \otimes \boldsymbol{W}_S + \boldsymbol{I}_T \otimes \boldsymbol{W}_S \tag{13}$$
in which:

$\boldsymbol{W}_S$: an $N \times N$ positive and symmetric matrix, with positive nonzero elements that indicate whether the two locations are neighbours. The following definition is commonly used:

$$w_{ij} = \begin{cases} 1, \text{ if } i \text{ and } j \text{ are neighbours} \\ 0, \text{ otherwise} \end{cases} \tag{14}$$
$$i, j = 1, \dots, N$$

Since a location cannot be its own neighbour, $\boldsymbol{W}_S$ has zero elements of its diagonal, and the symmetric property implies that $w_{ij} = w_{ji}$. The nature of interaction, i.e., attraction or repulsion forces between neighbours, depends on the assumed spatial autocorrelation. The first type is due to positive spatial autocorrelation such that neighbours have similar characteristics, whereas the latter is for negative spatial autocorrelation, which is indicated by dissimilar characteristics among neighbours.

$\boldsymbol{W}_T$: an $T \times T$ time weight matrix, with the elements:

$$t_{ij} = 0, \text{ for } i = j, i, j = 1, \dots, T$$

$$t_{ij} = \begin{cases} 1, \text{ if } |t_i - t_j| \leq tres \\ 0, \text{ if } |t_i - t_j| > tres \end{cases},$$

$$\text{for } i \neq j, i, j = 1, \dots, T \qquad (15)$$

t_i is the occurrence of the i-th observation, t_j is the occurrence of the j-th observation, and $tres$ is the time duration threshold ($tres = 1,2,3,\dots,T$), in which two observations with $tres$ time units apart still affect each other. The assumption regarding the choice of $tres$ depends on the nature of the observations. By definition, $\boldsymbol{W}_T$ has 0 on the main diagonal.

$\boldsymbol{I}_S$: an $N \times N$ identity matrix.

To maintain the property of the correlation index value (between –1 and 1), the space-time weight matrix in (13) needs to be unitized such that:

$$V^u = \frac{1}{g} [V_{ij}]_{NT \times NT}$$

$$g = \sum_{i=1}^{NT} \sum_{j=1}^{NT} V_{ij} \qquad (16)$$

Similar to the interpretation of a spatial lag variable (e.g., $\boldsymbol{WY}$, with row-normalized spatial weight matrix $\boldsymbol{W}$), as the average value of variable $\boldsymbol{Y}$ in the neighbouring locations, $\boldsymbol{V}^u \boldsymbol{Y}$ can be interpreted as a weighted effect of the current, previous and future periods of $\boldsymbol{Y}$ in the neighbouring regions.

The spatial cross-correlation index for time-dependent spatial panel data is then defined as:

$$R_c = \boldsymbol{x}^T \boldsymbol{V}^u \boldsymbol{y} = \boldsymbol{y}^T \boldsymbol{V}^u \boldsymbol{x} \qquad (17)$$

using the standardized spatial panel data vectors (in (3) and (4)) and the space-time weight matrix (in (16)). The index defined in (17) can be rearranged as follows:

$$\boldsymbol{x}^T \boldsymbol{V}^u \boldsymbol{y} \boldsymbol{x} = R_c \boldsymbol{x}$$

$$\boldsymbol{x}^T \boldsymbol{x} \boldsymbol{V}^u \boldsymbol{y} = R_c \boldsymbol{x} \qquad (18)$$

$$T(N-1) \boldsymbol{V}^u \boldsymbol{y} = R_c \boldsymbol{x}$$

where R_c is the slope of the trend line with $\boldsymbol{x}$ on the horizontal axis and $T(N-1)\boldsymbol{V}^u\boldsymbol{y}$ on the vertical axis. Alternatively, the index defined (17) can also be rearranged as:

$$\boldsymbol{y}^T \boldsymbol{V}^u \boldsymbol{x} \boldsymbol{y} = R_c \boldsymbol{y}$$
$$\boldsymbol{y}^T \boldsymbol{y} \boldsymbol{V}^u \boldsymbol{x} = R_c \boldsymbol{y} \qquad (19)$$
$$T(N-1)\boldsymbol{V}^u \boldsymbol{x} = R_c \boldsymbol{y}$$

in which R_c is the slope of the line between **y** in the horizontal axis and $T(N-1)\boldsymbol{V}^u\boldsymbol{x}$ in the vertical axis. Furthermore, it can also be shown mathematically that R_c is the least square estimator of the slope of regression between x and $T(N-1)\boldsymbol{V}^u\boldsymbol{y}$ without intercept:

$$R_c = \frac{\boldsymbol{x}^T T(N-1)\boldsymbol{V}^u \boldsymbol{y}}{\boldsymbol{x}^T \boldsymbol{x}}$$
$$= \frac{\boldsymbol{x}^T T(N-1)\boldsymbol{V}^u \boldsymbol{y}}{T(N-1)} \qquad (20)$$
$$= \boldsymbol{x}^T \boldsymbol{V}^u \boldsymbol{y}$$

or it is the least square estimator of the slope of regression between **y** and $T(N-1)\boldsymbol{V}^u\boldsymbol{x}$ without intercept:

$$R_c = \frac{\boldsymbol{y}^T T(N-1)\boldsymbol{V}^u \boldsymbol{x}}{\boldsymbol{y}^T \boldsymbol{y}}$$
$$= \frac{\boldsymbol{y}^T T(N-1)\boldsymbol{V}^u \boldsymbol{x}}{T(N-1)} \qquad (21)$$
$$= \boldsymbol{y}^T \boldsymbol{V}^u \boldsymbol{x}$$

In (20), it is assumed that the change in $\boldsymbol{x}$ leads to the change in $T(N-1)\boldsymbol{V}^u\boldsymbol{y}$. The opposite holds for (21), in which the change in $\boldsymbol{y}$ is assumed to be the cause of the change in $T(N-1)\boldsymbol{V}^u\boldsymbol{x}$. Thus, even though the calculation of the spatial cross-correlation index does not require a causal relationship between the two variables, different expressions of R_c in (20) and (21) indicate that the index can be used to identify the causal relationship. As a measure of correlation, the change in both variables can be in the same direction (positive correlation) or in the opposite direction (negative correlation). Mathematically, whether X or Y acts as the independent variable, the calculation leads to the same value of R_c. However, using regression analysis, each case yields a different coefficient of determination (R^2). The regression with larger R^2 is a better model.

The new index is used further for inference purposes. It is used to test the null hypothesis of independence between the current-local X vs. the current-neighbourhood Y as well as between the current X vs. the previous and the future neighbourhood Y. Analytically, the inference must be based on the theoretical distribution of the proposed index. Distribution of the index under the null hypothesis can be derived using the normality assumption or randomization. The first approach requires analytical derivations, which can be inappropriate when the normality assumption is violated. The second is based on a computational technique using permutation, which is more robust under nonnormality (Good 2013, Anselin et al. 2022). Since there is no guarantee that the normality assumption is satisfied, the distribution of the index in this study is derived using the second approach. Even

though the computational approach is considered a black box, it offers more advantages from a practical point of view. It is data driven and capable of handling large space-time datasets.

The permutation inference has been an alternative for obtaining the distribution of any statistics (Good 2013, Wheeler–Torchiano 2010, Pesarin–Salmaso 2010), which is used by several studies. Anselin et al. (2022) and Scrucca (2005) use the technique to obtain the distribution of Moran's I. In those studies, the inference regarding spatial randomness is made based on the pseudo p value. The pseudo p value is calculated based on a reference distribution of the index under no spatial cross-correlation. No spatial cross-correlation or spatially random cross-correlation means that the local value of X does not depend on the neighbourhood values of Y or vice versa. For that purpose, reshuffled datasets are created by randomly permuting the observed values of variable (X) over the locations. The index is then calculated for each dataset. Following the definition in Anselin (1995, 2001), the pseudo p value is defined as:

$$p = \frac{R + 1}{M + 1} \tag{22}$$

in which R is the frequency of the computed index from the permuted datasets, which are equal to or more than the absolute value of the observed index from the original dataset, and M is the number of permutations. M is usually set as 99, 999, etc.

Data and study area

East Java is one of the provinces in Indonesia, consisting of 38 regencies/municipalities. It is the main interest of this study because of its significant contribution to national economic growth (Fitriani et al. 2020, Solihin et al. 2021). From 2015–2019, the province had 9.6% economic growth on average, which is above the national growth (9.3%) (BPS 2021). The map of the administrative regions of the regencies/municipalities of the province is depicted in Figure 1.

The yearly (2014–2019) economic growth and percentage of urban population at the regency/municipality level are used. They are defined as:

X_{it}: GDP growth of regency/municipality i at year t and

Y_{it}: Percentage of urban population of regency/municipality i at year t,

$i = 1, \dots, 38, t = 2014, \dots, 2019$.

Both are secondary data provided by Indonesian Statistics Biro (*Badan Pusat Statistik*). Fitriani et al. (2023) showed the dynamics and spatial pattern of a region's economic growth.

Figure 1

Map of East Java's 38 regencies/municipalities
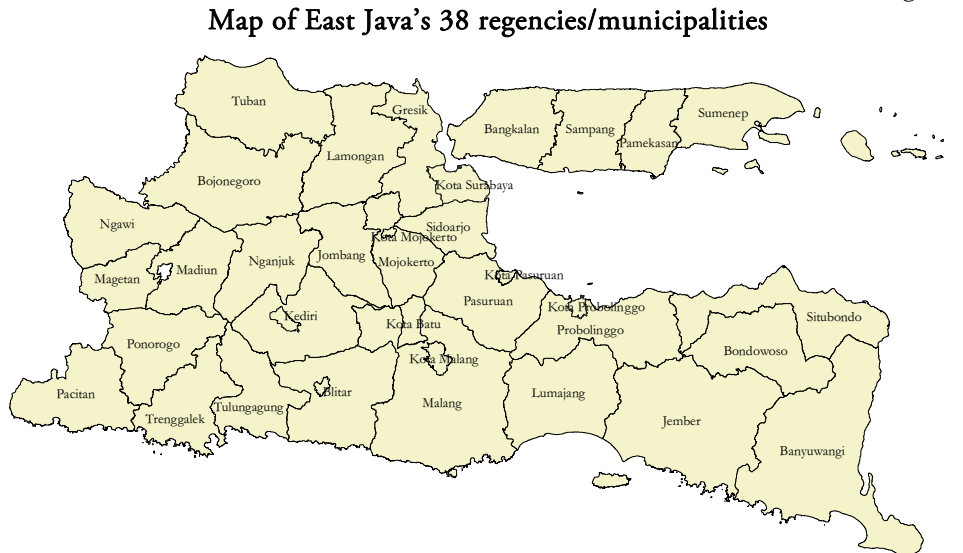
Simulation study

In this simulation study, it is assumed that two observations with one unit time lag have the strongest interaction, such that in (13) $tres = 1$.

The data generating setting

For data generating purposes, at time t, the following relations are assumed between two sets of spatial data, defined in $n \times 1$ vectors of $\boldsymbol{X}_t$ and $\boldsymbol{Y}_t$:

$$E(\boldsymbol{Y}_t) = \boldsymbol{\mu}_{Y_t}, var(\boldsymbol{Y}_t) = var(\boldsymbol{\varepsilon}) = \boldsymbol{\Sigma} = \sigma^2 \boldsymbol{I}_n$$
$$\boldsymbol{X}_t = \rho \boldsymbol{W} \boldsymbol{Y}_t,$$
$$E(\boldsymbol{X}_t) = \rho \boldsymbol{W} E(\boldsymbol{Y}_t), var(\boldsymbol{X}_t) = \boldsymbol{\Sigma}_X = \rho^2 \boldsymbol{W} var(\boldsymbol{Y}_t) \boldsymbol{W}^T = \rho^2 \sigma^2 \boldsymbol{W} \boldsymbol{W}^T.$$

In those relations, σ^2 is a parameter of variance, ρ is a parameter of spatial dependency, and $\boldsymbol{W}$ is a spatial weight matrix. These assumptions are used to generate vectors of $\boldsymbol{X}_t$ and $\boldsymbol{Y}_t$. The time dependence characteristic, however, needs to be accommodated in the data generation setting by defining the relation between $t - 1$ and t. Furthermore, several inputs are needed, namely:

$\boldsymbol{\mu}_{Y_0}$: an initial $n \times 1$ vector of mean of the first variable, which is defined from a variable of any secondary regional dataset.

$\sigma^2 = k \times S^2$: a variance parameter, in which k is the scale parameter of accuracy, and S^2 is the empirical variance of the secondary data used to define the mean vector.

In this study, the 2014 GDP growth of the 38 East Java regencies/municipalities $(GGDP_1, \ldots, GGDP_n, n = 38)$ is used to define $\boldsymbol{\mu}_{Y_0}$, and the variance of $GGDP_1, \ldots, GGDP_n, n = 38$ is used to define S^2. The spatial configuration of the 38

East Java regencies/municipalities is used to define the spatial weight matrix $\boldsymbol{W}$ based on the queen contiguity concept.

For the initial time, $t = 0$, the following relations hold:

$$Y_0 \sim N_n\left(\boldsymbol{\mu}_{Y_0}, \boldsymbol{\Sigma}\right)$$
$$X_0^A \sim N_n\left(\boldsymbol{\mu}_{X_0}, \boldsymbol{\Sigma}_X\right), \boldsymbol{\mu}_{X_0} = \rho \boldsymbol{W} Y_0,$$
$$\boldsymbol{\varepsilon}_0 \sim N_n(0, \boldsymbol{\Sigma}), \text{ and}$$
$$X_0 = X_0^A + \boldsymbol{\varepsilon}_0$$

For $t = 1,2,\ldots,T$, using the time autoregressive parameter ϕ, the following relations hold:

$$Y_t \sim N_n\left(\boldsymbol{\mu}_{Y_t}, \boldsymbol{\Sigma}\right), \boldsymbol{\mu}_{Y_t} = \phi \boldsymbol{\mu}_{Y_{t-1}},$$
$$X_t^A \sim N_n\left(\boldsymbol{\mu}_{X_t}, \boldsymbol{\Sigma}_X\right), \boldsymbol{\mu}_{X_t} = \rho \boldsymbol{W} Y_t,$$
$$\boldsymbol{\varepsilon}_t \sim N_n(0, \boldsymbol{\Sigma}), \boldsymbol{\mu}_{\varepsilon_t} = \phi \boldsymbol{\mu}_{\varepsilon_{t-1}} \text{ and}$$
$$X_t = X_t^A + \boldsymbol{\varepsilon}_t$$

In this study, 108 scenarios are used. They are combinations of several values of parameters ρ, ϕ and k:

$$\rho = -0.9, -0.5, -0.1, 0.1, 0.5, 0.9, \phi = -0.9, -0.5, -0.1, 0.1, 0.5, 0.9, k = 2, 1, 0.5$$

A smaller k leads to a more accurate relation between $\boldsymbol{X}$ and $\boldsymbol{Y}$. The spatial panel data are generated for 12 periods ($T = 12$). The range of parameter values ensures that the generated $\boldsymbol{X}$ and $\boldsymbol{Y}$ have both negative and positive time-dependent spatial cross-correlation.

Results and discussion

Properties of the modified time-dependent spatial cross-correlation index

The properties of R_c can be derived based on several types of space-time interdependence, which defines the space-time weight matrix in (12). Without losing generality, in this part, the space-time weight matrix is defined specifically by assuming that the strongest interaction is observed between two observations with 1 time unit apart.

(i) **In the presence of time and spatial dependence**, the space-time weight matrix is defined as:

$$\boldsymbol{V} = \boldsymbol{W}_T \otimes \boldsymbol{I}_N + \boldsymbol{I}_T \otimes \boldsymbol{I}_N$$

$$= \begin{bmatrix} 0 & \boldsymbol{I}_N & 0 & 0 & \ldots & 0 & 0 \\ \boldsymbol{I}_N & 0 & \boldsymbol{I}_N & 0 & \ldots & 0 & 0 \\ 0 & \boldsymbol{I}_N & 0 & \boldsymbol{I}_N & \ldots & 0 & 0 \\ 0 & 0 & \boldsymbol{I}_N & 0 & \ldots & 0 & 0 \\ \vdots & \vdots & \vdots & \vdots & \ddots & \vdots & \vdots \\ 0 & 0 & 0 & 0 & \ldots & 0 & \boldsymbol{I}_N \\ 0 & 0 & 0 & 0 & \ldots & \boldsymbol{I}_N & 0 \end{bmatrix} + \begin{bmatrix} \boldsymbol{I}_N & 0 & 0 & 0 & \ldots & 0 & 0 \\ 0 & \boldsymbol{I}_N & 0 & 0 & \ldots & 0 & 0 \\ 0 & 0 & \boldsymbol{I}_N & 0 & \ldots & 0 & 0 \\ 0 & 0 & 0 & \boldsymbol{I}_N & \ldots & 0 & 0 \\ \vdots & \vdots & \vdots & \vdots & \ddots & \vdots & \vdots \\ 0 & 0 & 0 & 0 & \ldots & 0 & 0 \\ 0 & 0 & 0 & 0 & \ldots & 0 & \boldsymbol{I}_N \end{bmatrix}$$

By setting $k = \sum_{i=1}^{T} \sum_{j=1}^{T} w_{T,ij}$, $T = \sum_{i=1}^{T} \sum_{j=1}^{T} I_{T,ij}$, and $N = \sum_{i=1}^{T} \sum_{i=1}^{T} I_{N,ij}$, the unitized space-time weight matrix can be defined as:

$$\boldsymbol{V}^u = \frac{1}{(k+T)}\big[V_{ij}\big]_{NT \times NT}$$

Using the defined space-time weight matrix, the spatial cross-correlation index can be elaborated as:

$$R_c = \boldsymbol{x}^T \boldsymbol{V}^u \boldsymbol{y} = \frac{1}{(k+T)N}\big(\boldsymbol{x}^T(\boldsymbol{W}_T \otimes \boldsymbol{I}_N)\boldsymbol{y} + \boldsymbol{x}^T(\boldsymbol{I}_T \otimes \boldsymbol{I}_N)\boldsymbol{y}\big)$$

which is the weighted sum of two components: 1) correlation between x_t vs. y_{t-1} and x_t vs. y_{t+1} and 2) the panel version of correlation between x_t vs. y_t

(ii) **In the presence of spatial dependence with no time dependence**, the space-time weight matrix is defined as follows:

$$\boldsymbol{V} = \boldsymbol{I}_T \otimes \boldsymbol{W}_S = \begin{bmatrix} \boldsymbol{W}_S & 0 & \dots & 0 \\ 0 & \boldsymbol{W}_S & \dots & 0 \\ \vdots & \vdots & \ddots & 0 \\ 0 & 0 & \dots & \boldsymbol{W}_S \end{bmatrix}$$

By setting $s = \sum_{i=1}^{N} \sum_{i=1}^{N} w_{S,ij}$, the unitized space-time weight matrix is defined as

$$\boldsymbol{V}^u = \frac{1}{sT}\big[V_{ij}\big]_{NT \times NT}$$

Using the defined space-time weight matrix, the spatial cross-correlation index is then elaborated such that:

$$R_c = \boldsymbol{x}^T \boldsymbol{V}^u \boldsymbol{y} = \frac{1}{sT}\big(\boldsymbol{x}_1^T \boldsymbol{W}_s \boldsymbol{y}_1 + \boldsymbol{x}_2^T \boldsymbol{W}_s \boldsymbol{y}_2 + \dots + \boldsymbol{x}_T^T \boldsymbol{W}_s \boldsymbol{y}_T\big)$$

in which $\boldsymbol{x}_t, \boldsymbol{y}_t, t = 1, \dots, T$, are the vectors of variables observed at time t across locations. In this case, the index becomes the weighted sum Chen's spatial cross-correlation index for all t.

(iii) **When there is no time and no spatial dependence**, the space-time weight matrix is defined as follows:

$$\boldsymbol{V} = \boldsymbol{I}_T \otimes \boldsymbol{I}_N = \begin{bmatrix} \boldsymbol{I}_N & 0 & \dots & 0 \\ 0 & \boldsymbol{I}_N & \dots & 0 \\ \vdots & \vdots & \ddots & 0 \\ 0 & 0 & \dots & \boldsymbol{I}_N \end{bmatrix}$$

and the unitized space-time weight matrix is defined as:

$$\boldsymbol{V}^u = \frac{1}{NT}\big[V_{ij}\big]_{NT \times NT}$$

Accordingly, the spatial cross-correlation index becomes:

$$R_c = \boldsymbol{x}^T \boldsymbol{V}^u \boldsymbol{y} = \frac{1}{NT}\big(\boldsymbol{x}_1^T \boldsymbol{I}_N \boldsymbol{y}_1 + \boldsymbol{x}_2^T \boldsymbol{I}_N \boldsymbol{y}_2 + \dots + \boldsymbol{x}_T^T \boldsymbol{I}_N \boldsymbol{y}_T\big)$$

in which $\boldsymbol{x}_t, \boldsymbol{y}_t, t = 1, \dots, T$, are the vectors of variables observed at time t across locations. The index becomes the weighted sum of Pearson correlation for all t.

In addition to the above properties, when the index is applied to the same variables without time dependence, the space-time weight matrix becomes:

$$V = I_T \otimes W_S = \begin{bmatrix} W_S & 0 & \dots & 0 \\ 0 & W_S & \dots & 0 \\ \vdots & \vdots & \ddots & 0 \\ 0 & 0 & \dots & W_S \end{bmatrix}$$

Using $s = \sum_{i=1}^{N} \sum_{j=1}^{N} w_{S,ij}$, the unitized space-time weight matrix is defined as:

$$V^u = \frac{1}{sT} [V_{ij}]_{NT \times NT}$$

Consequently, the index can be represented as:

$$R_c = x^T V^u x = \frac{1}{NT} (x_1^T W_S x_1 + x_2^T W_S x_2 + \dots + x_T^T W_S x_T),$$

the weighted sum of Moran's index for all t.

Pattern of generated data

The nature of the spatial panel dataset produced by the data generation setting will be shown in the following section. Time series plots of Y for the first 4 locations are presented to visualize the time dynamics of Y. The scatter plot between neighbourhood Y (WY) and local X for the first four periods is used to describe the correlation between them. The plots are presented only for some scenarios (combinations between the values of ρ, ϕ and k).

Combination of $\rho = 0.1, \phi = 0.1, k = 2$

This scenario represents the weakest positive space-time dependence and the least accurate relationship between X and Y. The time series plots for the generated Y are depicted in Figure 2. The plots indicate a slight time dependence. The scatter plots between the generated neighbourhood Y (WY) and local X for the first four periods are depicted in Figure 3. Each plot shows no apparent trend. This is a plausible result due to the choice of parameter values.

Figure 2

The time series of the generated Y using a combination of
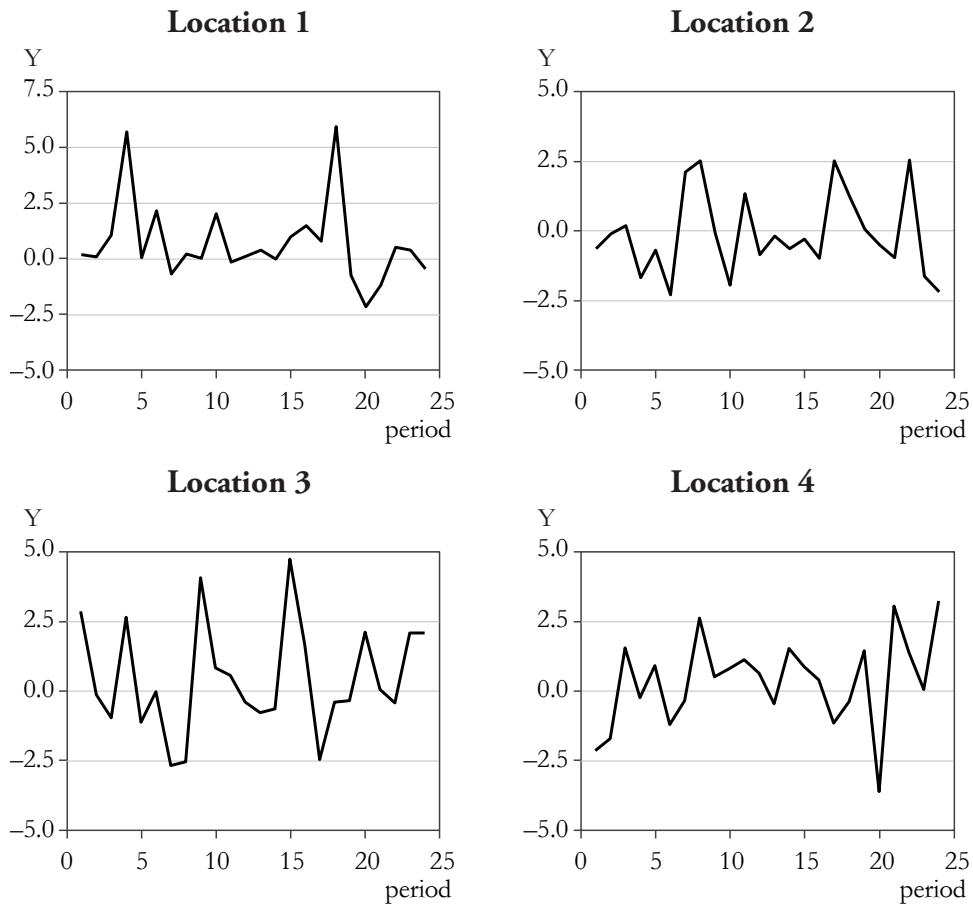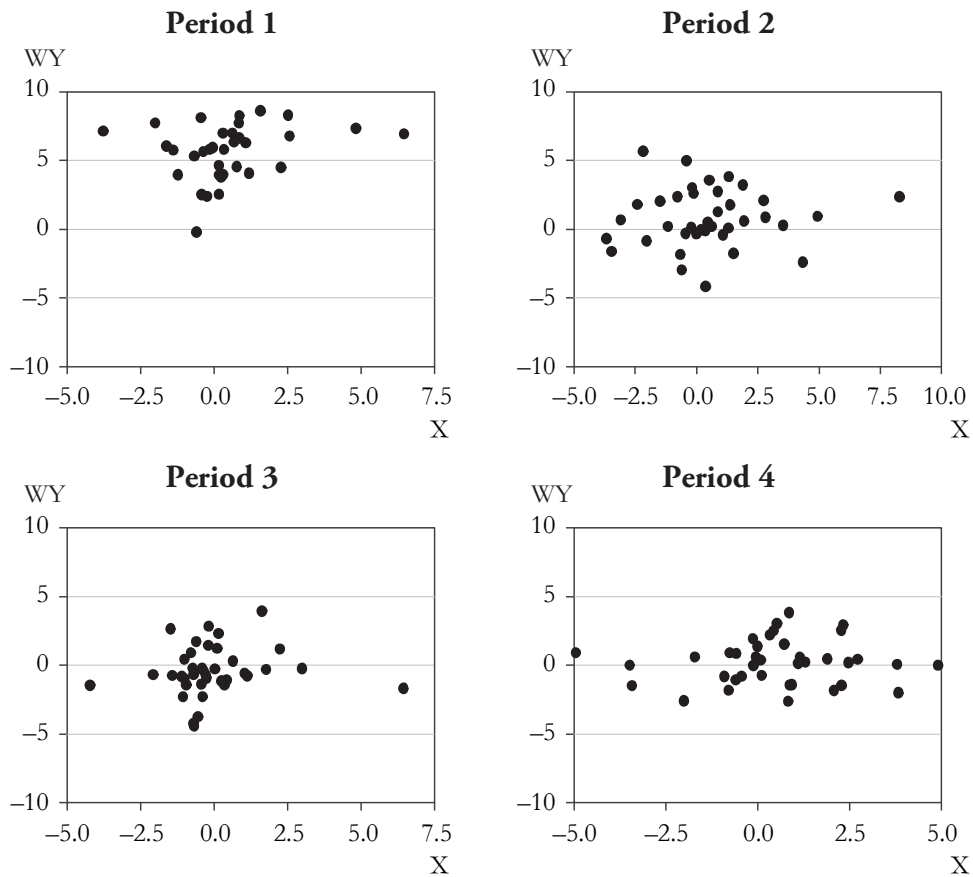**$\rho = 0.1, \phi = 0.1, k = 2$ for the first four locations**

Figure 3

Scatter plots between the generated neighbourhood Y (WY) and local X for the first four periods using a combination of $\rho = 0.1, \phi = 0.1, k = 2$

Combination of $\rho = 0.9, \phi = 0.9, k = 0.5$

This combination defines a scenario for the strongest positive space-time dependence and the most accurate relation between X and Y. The apparent time dependence of the generated Y is shown by the time series plots in Figure 4. The scatter plots between neighbourhood Y (WY) and local X for the first four periods are depicted in Figure 5. The plots indicate a strong positive relation between the two variables.

Figure 4

The time series of the generated *Y* using a combination of
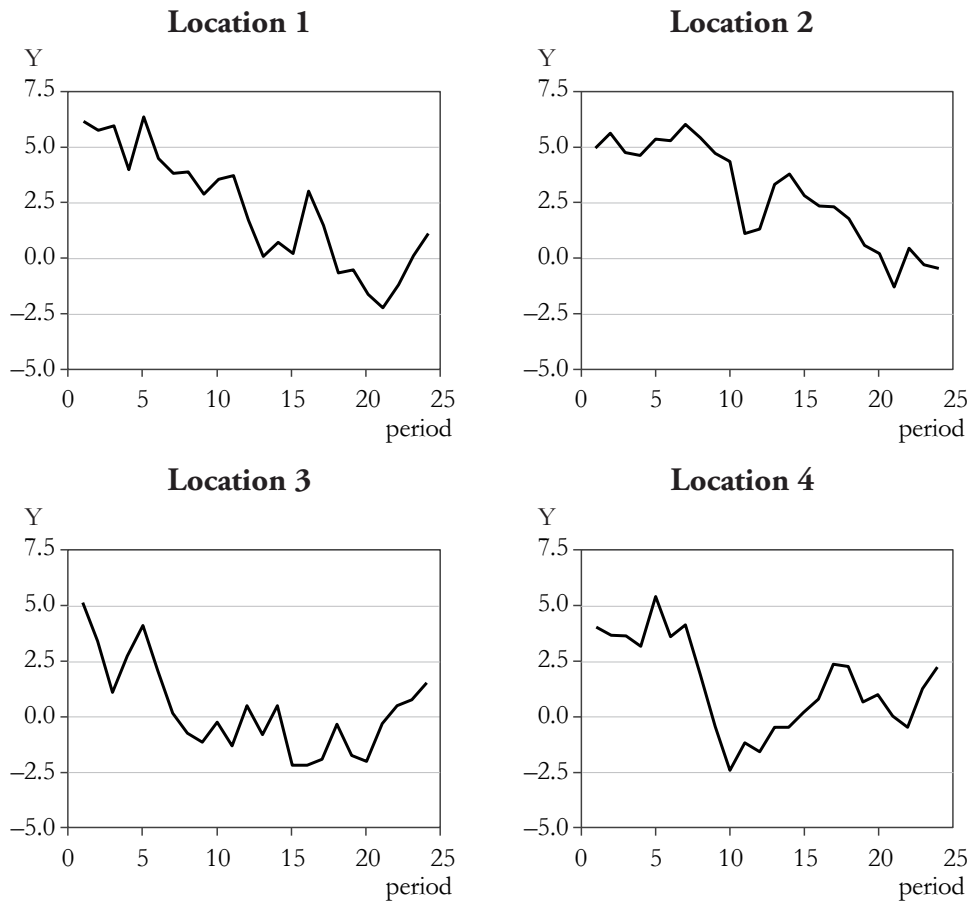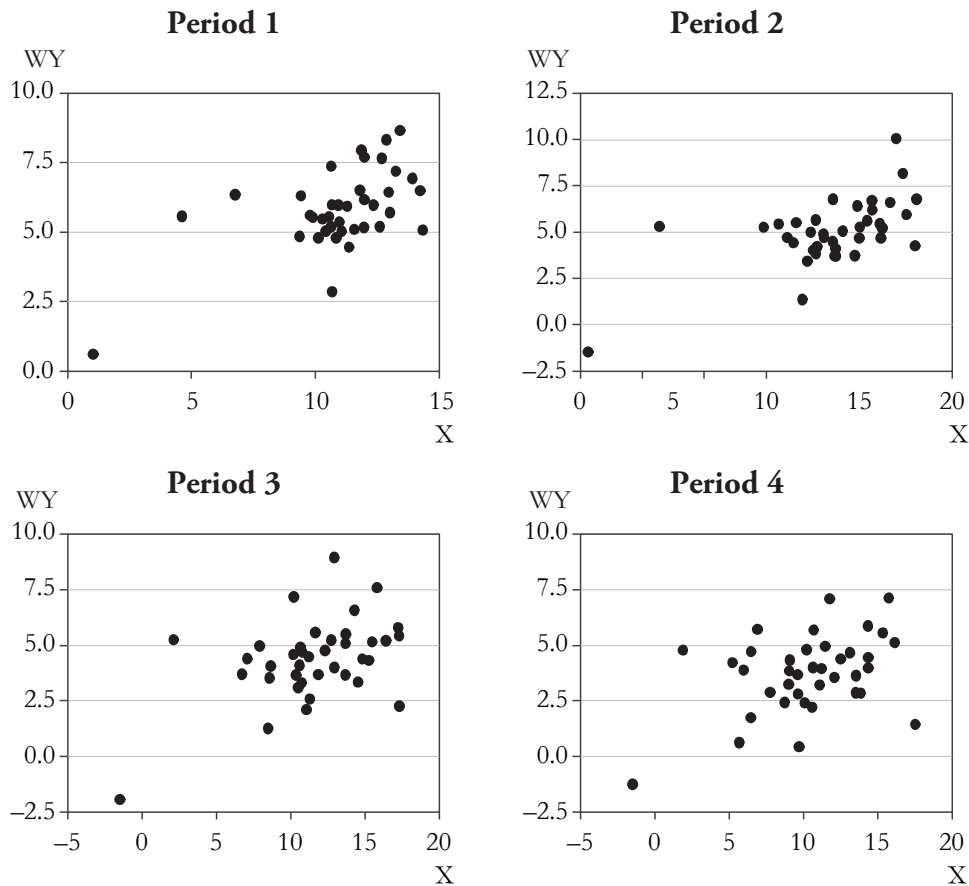**$\rho = 0.9, \phi = 0.9, k = 0.5$ for the first four locations**

Figure 5

Scatter plots between the generated neighbourhood Y (WY) and local X for the first four periods using a combination of $\rho = 0.9, \phi = 0.9, k = 0.5$

Combination of $\rho = -0.9, \phi = 0.9, k = 0.5$

This combination represents extremely opposite movement between the values of local **X** and the values of neighbourhood **Y** (**WY**), which allows similar values for those variables across time (strong positive autocorrelation), at the most accurate relation between **X** and **Y**. Time series plots for generated **Y** for the first four locations are presented in Figure 6. The trend observed in Figure 6 is not as smooth as the trend observed in Figure 4 when $\rho > 0$ and $\phi > 0$. The scatter plots in Figure 7 indicate that initially, the neighbourhood **Y** (**WY**) and local **X** have a strong negative correlation. The degree of correlation, however, slightly decreases over time.

Figure 6

The time series of the generated Y using a combination of $\rho = -0.9, \phi = 0.9, k = 0.5$ for the first four locations
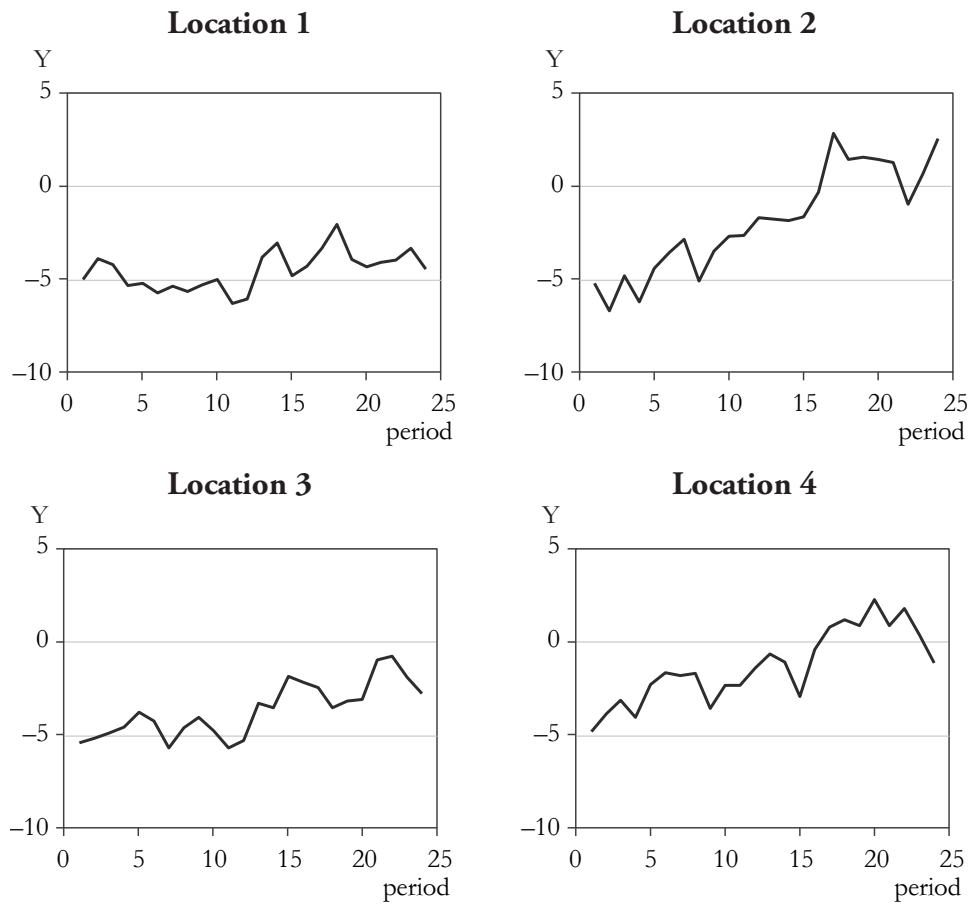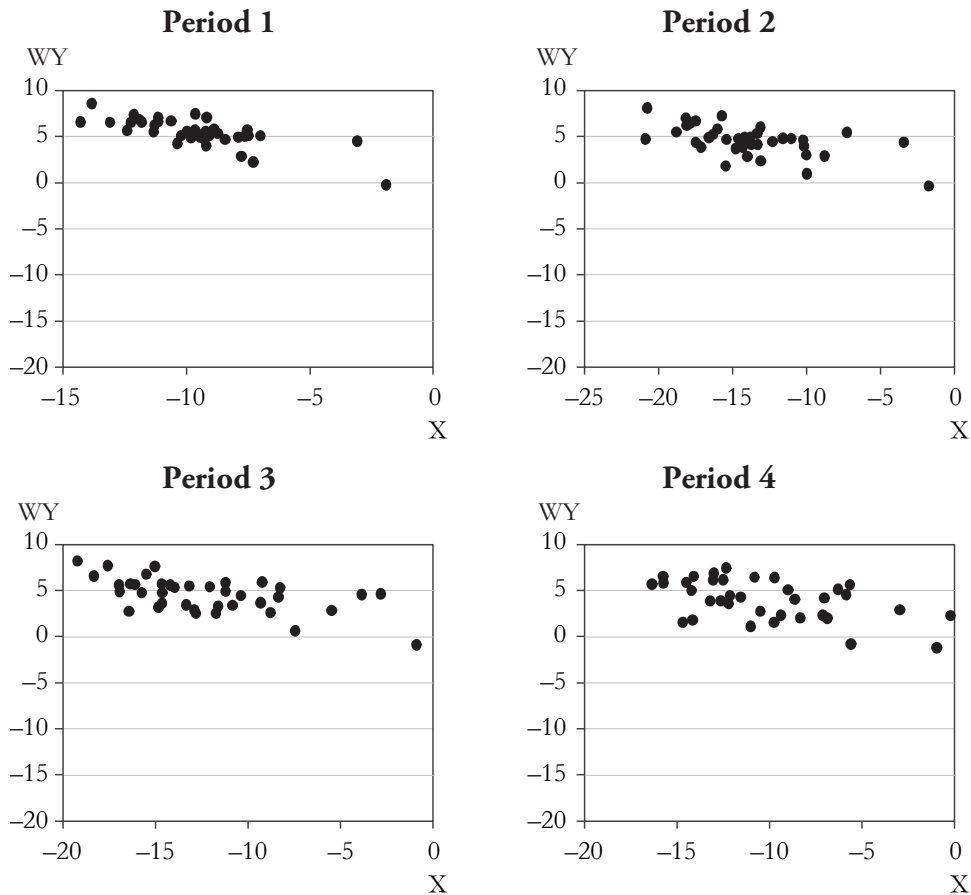

Location 1

Location 2

Location 3

Location 4

The scatter plots between the generated neighbourhood Y (WY) and local X using a combination of $\rho = -0.9, \phi = 0.9, k = 0.5$

Combination of $\rho = 0.9, \phi = -0.9, k = 0.5$

This scenario captures similar movement between the values of local $\boldsymbol{X}$ and the values of neighbourhood local $\boldsymbol{Y}$ ($\boldsymbol{WY}$) and opposite directions of movement across time between those variables, with the most accurate relation between $\boldsymbol{X}$ and $\boldsymbol{Y}$. Time series plots for generated $\boldsymbol{Y}$ for the first four locations are presented in Figure 8. Each plot in Figure 8 does not show a trend over time. The scatter plots in Figure 9 indicate a negative correlation between neighbourhood $\boldsymbol{Y}$ ($\boldsymbol{WY}$) and local $\boldsymbol{X}$, with an increasing degree over time.

The time series of the generated Y using
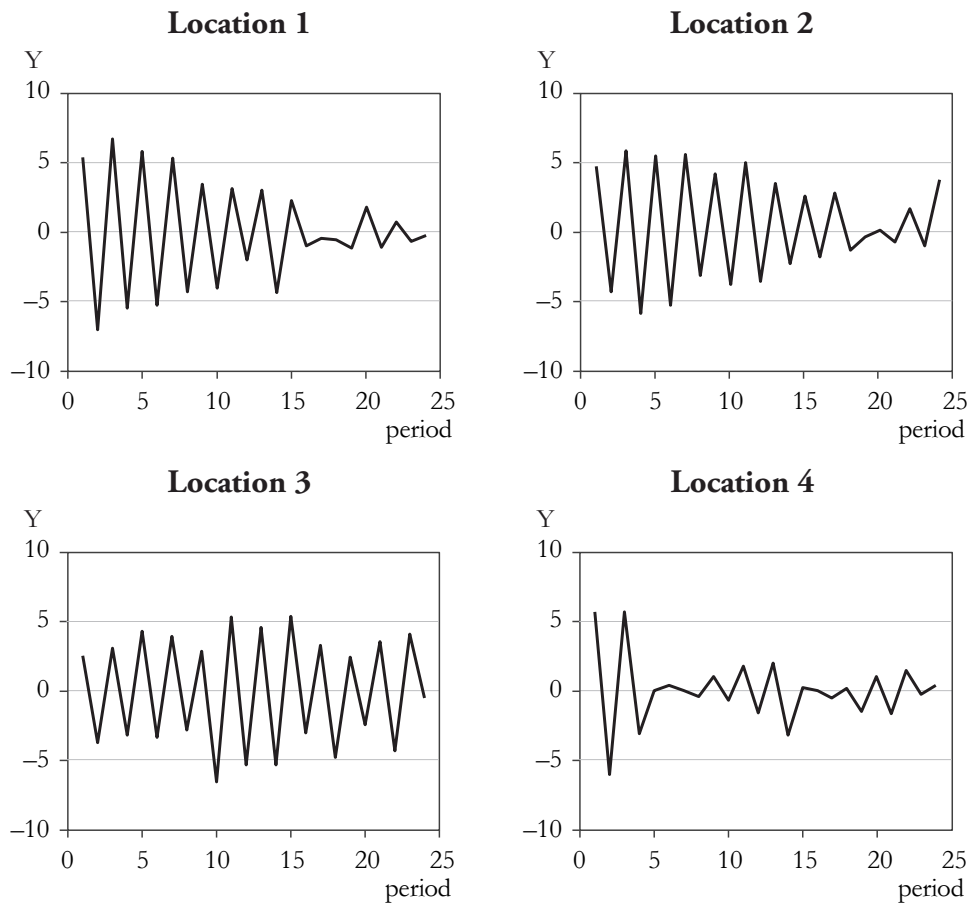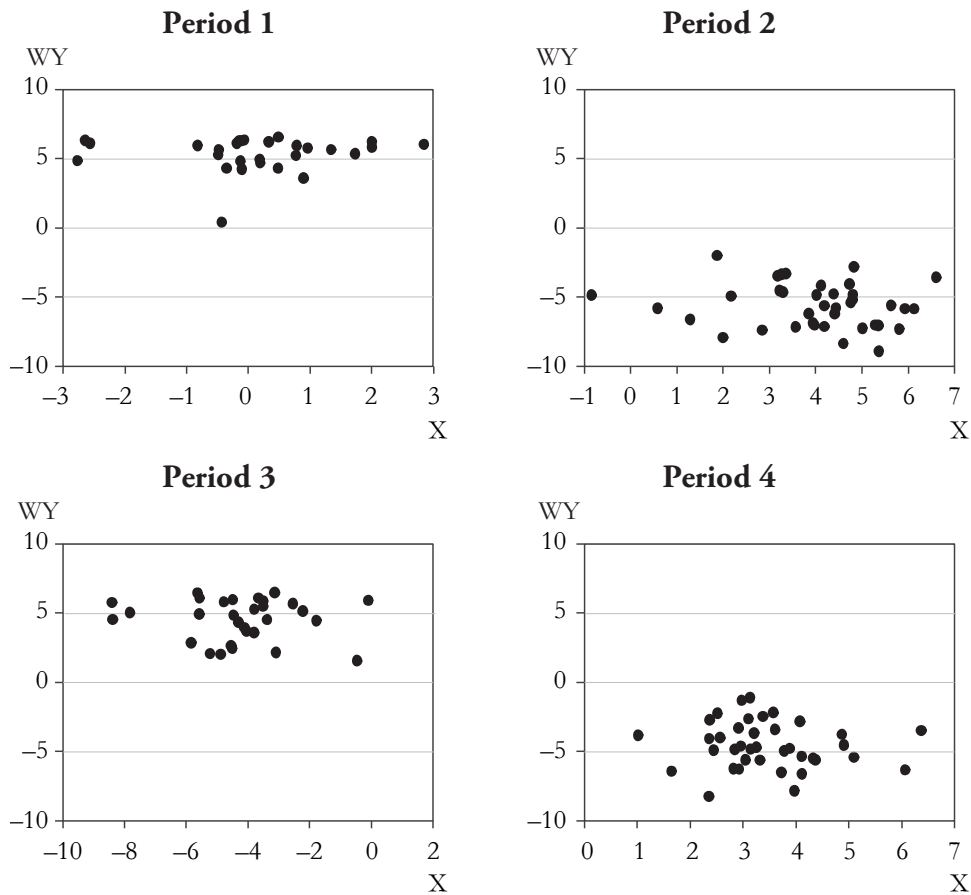## a combination of $\rho = 0.9, \phi = -0.9, k = 0.5$ for the first four locations

The scatter plots between the generated neighbourhood Y (WY) and local X using a combination of $\rho = 0.9, \phi = -0.9, k = 0.5$

Period 1   **Period 2**

Period 3   **Period 4**

Combination of $\rho = -0.9, \phi = -0.9, k = 0.5$

This combination of parameters is a scenario that captures opposite movement between the values of local X and the values of neighbourhood Y (WY) and opposite directions of movement across time between those variables at the most accurate relation between X and Y. The time series plots in Figure 10 are the typical pattern of time series with negative autocorrelation. The scatter plots between neighbourhood Y (WY) and local X for the first four periods are depicted in Figure 11. The plots indicate a strong positive relation between the two variables.

The time series of the generated Y using a combination of $\rho = -0.9, \phi = -0.9, k = 0.5$ for the first four locations
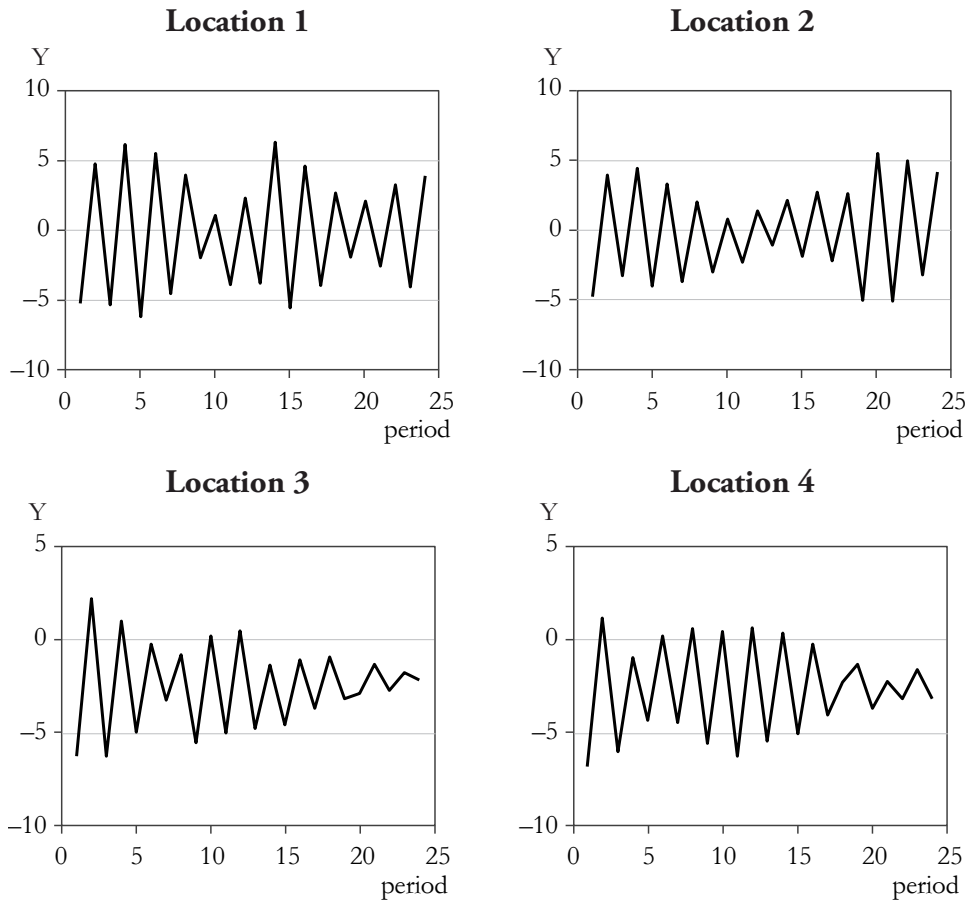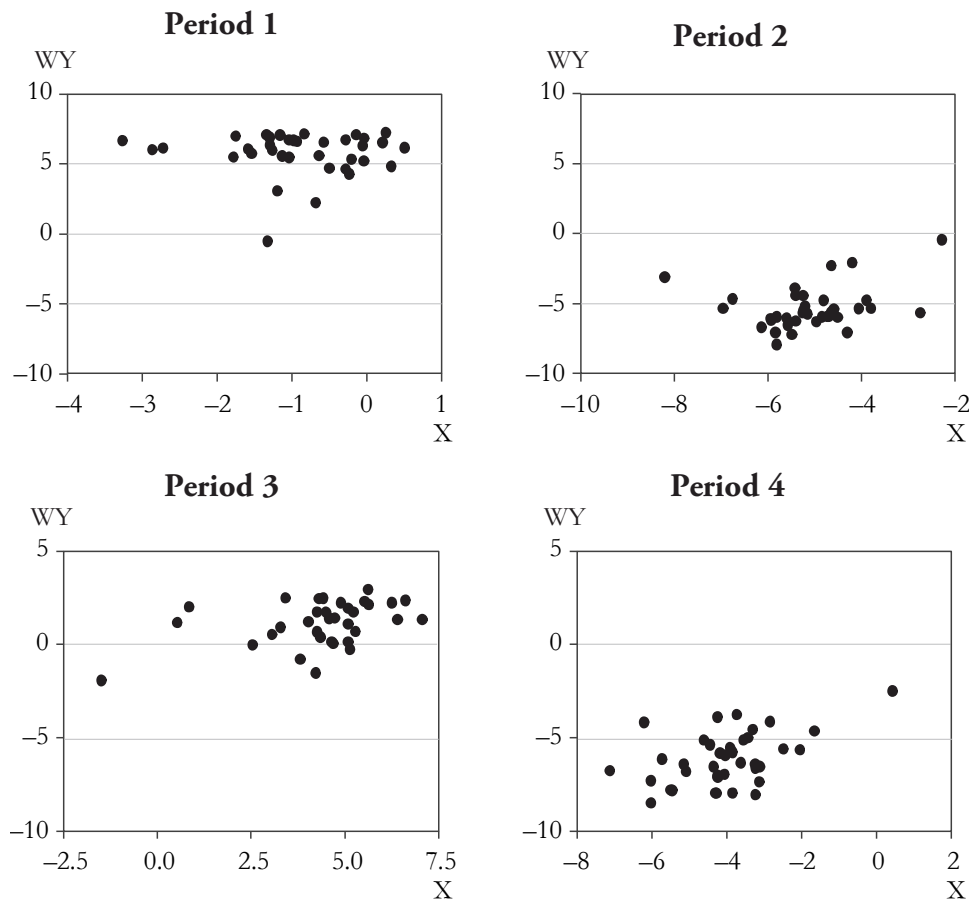
Figure 11

The scatter plots between the generated neighbourhood Y (WY) and local X using a combination of $\rho = -0.9, \phi = -0.9, k = 0.5$

Without presenting the plots of the generated data under the rest of the scenarios, this study confirms the effectiveness of the data generation setting to produce the spatial panel of X and Y with several degrees of negative/positive time-dependent spatial cross-correlation. Combinations of $\rho > 0$ and $\phi > 0$ or $\rho < 0$ and $\phi < 0$ generate X and Y with positive time-dependent spatial cross-correlation, whereas combinations of $\rho < 0$ and $\phi > 0$ or $\rho > 0$ and $\phi < 0$ produce X and Y with negative time-dependent spatial cross-correlation.

Table 1

Percentage of datasets with significant R_c
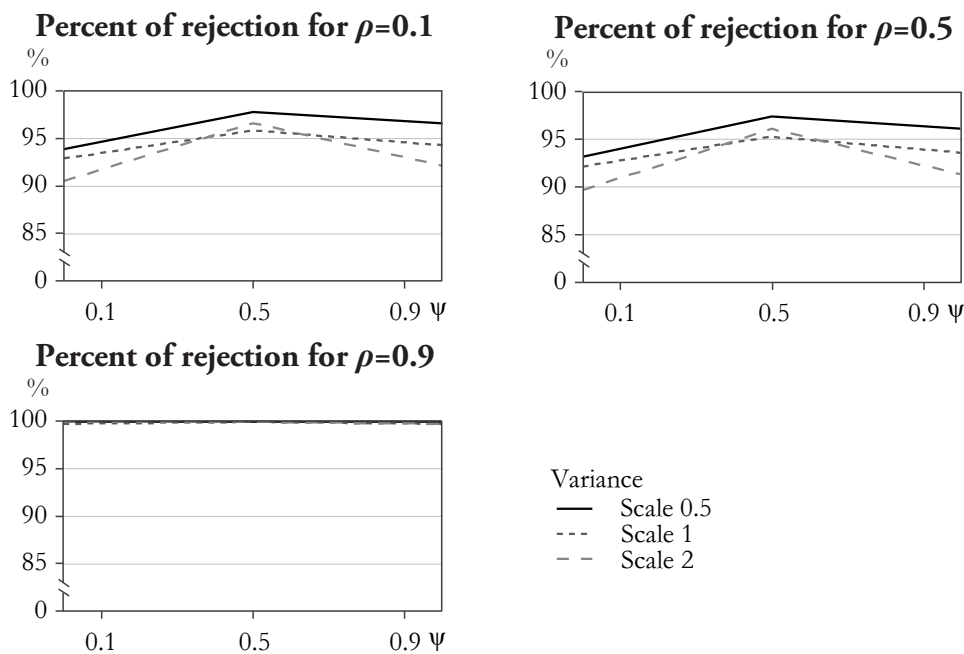**for combinations of $\rho > 0$ and $\phi > 0$**

ϕ	$k = 1$			$k = 0.5$			$\rho = 0.9$		
	$k = 2$	$k = 1$	$k = 0.5$	$k = 2$	$k = 1$	$k = 0.5$	$k = 2$	$k = 1$	$k = 0.5$
0.1	18.8	16.2	25.4	91.2	93.6	94.6	100.0	99.8	100.0
0.5	32.0	33.8	33.2	97.4	96.6	98.6	100.0	100.0	100.0
0.9	40.8	42.6	42	92.8	95.0	97.4	99.8	99.8	100.0

Performance of the index based on the simulation study

For each of the 108 scenarios, 500 sets of spatial panel data are generated. The index R_c in (17) and pseudo p value in **(22)** are calculated for each dataset. For each scenario, the accuracy of the index is analysed based on the percentage datasets (from 500) with significant R_c. The results are summarized in Table 1 through Table 4. The visualization of the results is also depicted in Figure 12 through Figure 15.

Figure 12

Percentage of datasets with significant R_c
for scenarios with combinations of $\rho > 0$ and $\phi > 0$

The results for combinations of $\rho > 0$ and $\phi > 0$, which generate $\boldsymbol{X}$ and $\boldsymbol{Y}$ with positive time-dependent spatial cross-correlation, are presented in Table 1. They indicate that in the presence of weak spatial dependence (of $\rho = 0.1$), the index can detect 16%–25% of datasets with significant spatial cross-correlation. The percentage increases when the degree of time dependence is stronger. For medium and strong degrees of spatial dependence ($\rho = 0.5$ and $\rho > 0.9$), the index can detect more than 90% of datasets with significant R_c. The highest percentage is observed in several scenarios, including the scenario with the strongest time-spatial dependence and the highest accuracy.
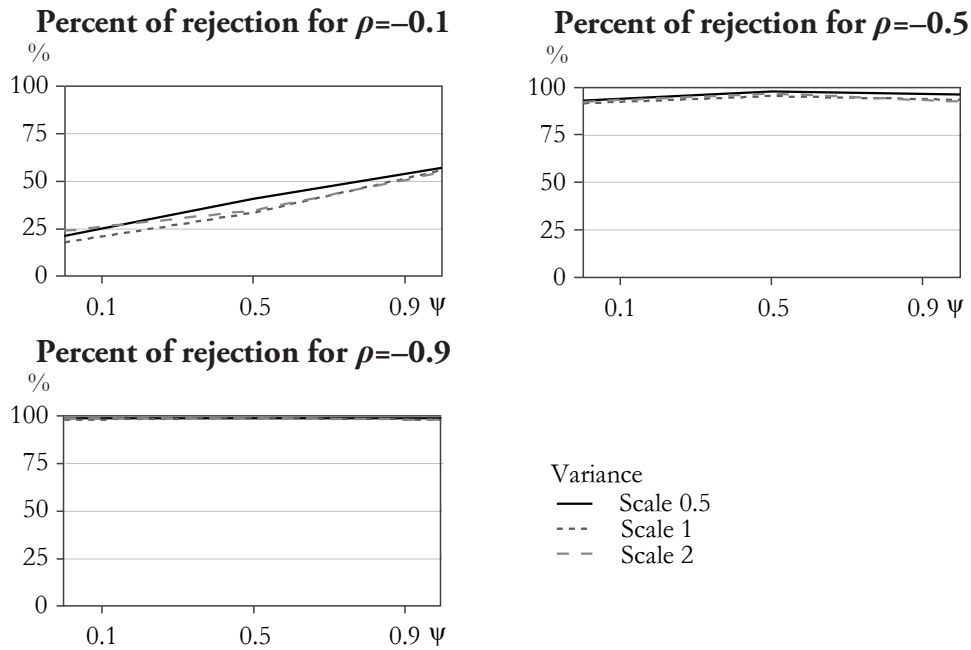
Table 2

Percentage of datasets with significant R_c
for combinations of $\rho < 0$ and $\phi > 0$

ϕ	$k = 1$			$k = 0.5$			$\rho = 0.9$		
	$k = 2$	$k = 1$	$k = 0.5$	$k = 2$	$k = 1$	$k = 0.5$	$k = 2$	$k = 1$	$k = 0.5$
0.1	23.4	17.2	20.8	93.4	92.6	94.0	99.8	100.0	100.0
0.5	34.2	33.0	40.2	97.8	96.4	98.8	100.0	100.0	100.0
0.9	54.4	55.6	57.0	93.4	94.4	97.2	100.0	100.0	100.0

The results for combinations of $\rho < 0$ and $\phi > 0$, generate $\boldsymbol{X}$ and $\boldsymbol{Y}$ with negative time-dependent spatial cross-correlation are presented in Table 2. The results are similar to those for scenarios with $\rho > 0$ and $\phi > 0$. The percentage of datasets with significant R_c increases with the increasing degree of spatial and time dependence. Only when the spatial dependence is weak ($\rho = -0.1$) is the percentage quite low (17.2%–57%). For medium and strong degrees of spatial dependence ($\rho = -0.5$ and $\rho = -0.9$), the index can detect more than 90% of datasets with significant R_c. The index (R_c) can detect 100% negative time-dependent spatial cross-correlation in almost every combination with strong spatial dependence ($\rho = -0.9$).

Figure 13

Percentage of datasets with significant R_c
for scenarios with combinations of $\rho < 0$ and $\phi > 0$

Percent of rejection for ρ=–0.1

Percent of rejection for ρ=–0.5

Percent of rejection for ρ=–0.9

Variance
—— Scale 0.5
- - - Scale 1
– – Scale 2

Combinations of $\rho > 0$ and $\phi < 0$ also generate $\boldsymbol{X}$ and $\boldsymbol{Y}$ with negative time-dependent spatial cross-correlation. The results of the simulation study for these scenarios are depicted in Table 3. As expected, the combinations for weak spatial dependence ($\rho = 0.1$) yield the lowest percentage of datasets with significant R_c (7.6%–46.8%). Every combination with a medium degree of time dependence has the lowest percentage of datasets with a significant R_c (7.6%–11.2%). Although the percentage increases as the degree of spatial dependence increases, there is no combination with 100% of the datasets that are significant R_c. The highest percentage is only 98%, for the highest degree of spatial and (negative) time dependence.

Table 3

Percentage of datasets with significant R_c for combinations of $\rho > 0$ and $\phi < 0$

ϕ	$k = 1$			$k = 0.5$			$\rho = 0.9$		
	$k = 2$	$k = 1$	$k = 0.5$	$k = 2$	$k = 1$	$k = 0.5$	$k = 2$	$k = 1$	$k = 0.5$
–0.1	14.2	12.0	15.4	78.6	78.8	85.4	96.0	97.4	97.8
–0.5	7.8	7.6	10.2	8.0	10.4	9.2	10.0	9.6	11.2
–0.9	39.2	46.8	45.0	76.4	80.6	84.6	93.2	95.6	98.0

Figure 14

Percentage of datasets with significant R_c
for scenarios with combinations of $\rho > 0$ and $\phi < 0$

Percent of rejection for ρ=0.1

Percent of rejection for ρ=0.5

Percent of rejection for ρ=0.9

Variance
— Scale 0.5
- - - Scale 1
– – Scale 2

Table 4

Percentage of datasets with significant R_c
for combinations of $\rho < 0$ and $\phi < 0$
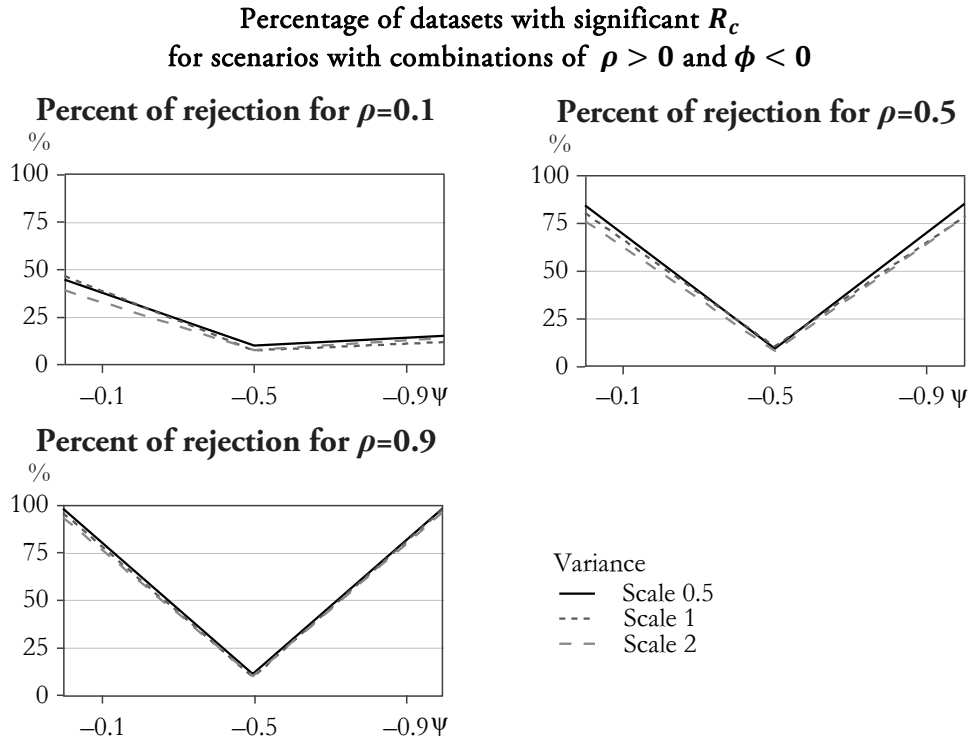
ϕ	$k = 1$			$k = 0.5$			$\rho = 0.9$		
	$k = 2$	$k = 1$	$k = 0.5$	$k = 2$	$k = 1$	$k = 0.5$	$k = 2$	$k = 1$	$k = 0.5$
−0.1	13.2	10.6	15.6	78.0	80.4	83.8	98.0	96.8	97.6
−0.5	8.0	9.4	7.0	7.0	10.2	7.8	12.0	9.2	9.0
−0.9	39.4	39.6	45.6	73.6	81.4	84.8	92.8	96.8	96.8

The second combination, which generates X and Y with positive time-dependent spatial cross-correlation, uses $\rho < 0$ and $\phi < 0$ in the data generation setting. The results of the simulation study for these combinations are presented in Table 4. The combinations for weak spatial dependence ($\rho = -0.1$) yield the lowest percentage of datasets with significant R_c (7%–45.6%). Every combination with a medium degree of time dependence has the lowest percentage of datasets with significant R_c (7%–12%). Similar to the results of the previous combination, even though the percentage

increases as the degree of spatial dependence increases, there is no combination with 100% datasets that are significant R_c. The highest percentage is only 98%.

Figure 15

Percentage of datasets with significant R_c for scenarios with combinations of $\rho < 0$ and $\phi < 0$

Percent of rejection for ρ=–0.1

Percent of rejection for ρ=–0.5

Percent of rejection for ρ=–0.9

Variance
— Scale 0.5
--- Scale 1
– – Scale 2
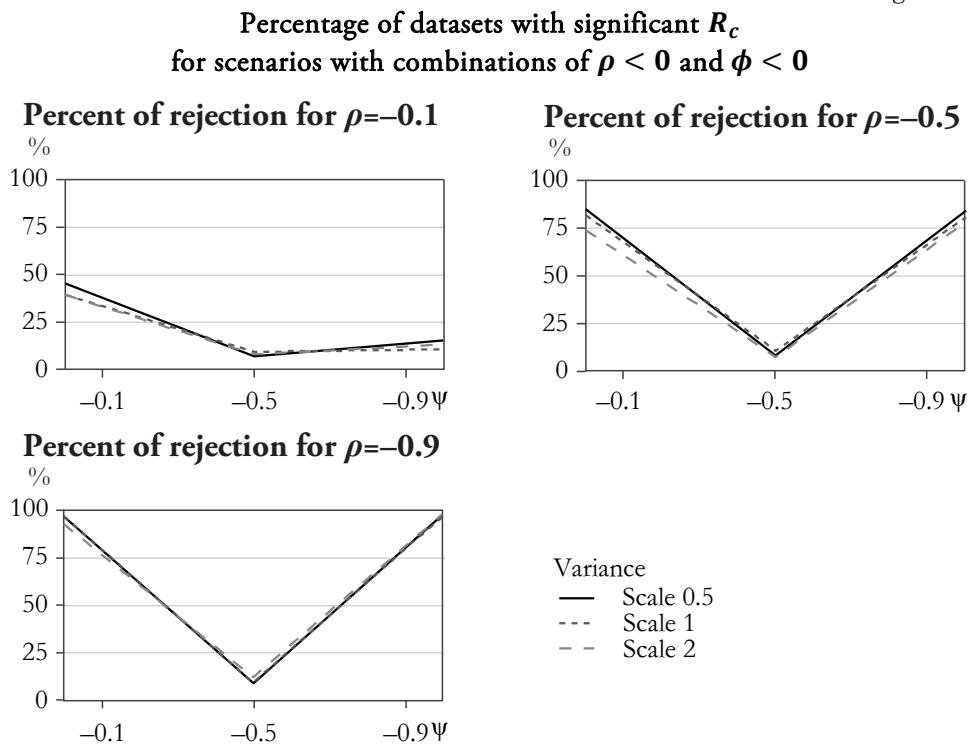
The simulation study shows that in the presence of at least moderate positive or negative spatial dependence, the modified index R_c can accurately detect the positive as well as the negative time-dependent spatial cross-correlation between **X** and **Y**. The best performance of the index is observed when the time series of every individual spatial unit has positive autocorrelation (positive time dependence) and the neighbourhood **Y** (**WY**) and local **X** of every time unit are positively correlated (positive spatial dependence). To understand well the pattern of time series and the spatial data, the application of this index can be accompanied by presenting data visualization.

The application of the index for East Java's regional GDP growth vs. percentage of urban population, 2015–2019

When the index is applied to calculate the time-dependent spatial cross-correlation between East Java's regional GDP growth and the percentage of urban population, the magnitude of the index and its significance represent two things:

1. the strength of the relationship between the current GDP growth of a regency/municipality and the current neighbourhood percentage of the urban population as well as the previous and the next year neighbourhood percentage of the urban population.
2. The strength of the relationship between the current percentage of urban population of a regency/municipality and the current neighbourhood GDP growth as well the previous and the next year neighbourhood GDP growth.

They both do not consider the causal-effect relationship.

The space-time weight matrix in (13) is formed using W_S, a spatial contiguity weight matrix that is defined based on the geographical location of the 38 East Java regencies/municipalities, and W_T with one year as the time threshold. The results are presented in Table 5. Due to the symmetric space-time weight matrix in the index development (Chen 2013), in both cases, the magnitudes of the index are the same. However, because of the setting of the randomization in the pseudo p value calculation (equation [22]), the p value of each case is different. At the 10% significance level, the results in Table 5 confirm that, for the 38 East Java regencies/municipalities (2014–2019 data), the time-dependent spatial cross-correlation between regional GDP growth and urbanization is significant.

Table 5

The time-dependent spatial cross-correlation index, the value and its significant for two possible relationships for GDP growth and urbanization of the 38 East Java regencies/municipalities (2014–2019 data)

Measure	GDP growth vs. space time lag of percentage of urban population	Percentage of urban population vs. space time lag of GDP growth
R_c	0.0425312	0.0425312
p value	0.083	0.081
R^2	0.0067824	0.0089617

Mathematically, R_c is the least square estimate of regression without an intercept between x and $T(N-1)V^u y$ or between y and $T(N-1)V^u x$; therefore, it is also useful to identify the causal relationship between two variables, GDP growth and the percentage of the urban population of the 38 East Java regencies/municipalities in this case. Two scatter plots are presented in Figure 15 to visualize the relationship between one variable locally and the space-time lag (multiplied by a constant) of another variable. In both cases, the value in the y-axis is the product of $T(N-1)$, the space-time weight matrix in (13) and the variable of interest. The first plot (the left panel of Figure 15) is made based on the assumption that the change in local GDP growth (the x-axis) drives the change in the space-time lag of the percentage of urban population (the y-axis). The plot shows that most of the regencies/municipalities have approximately 5% GDP growth. This cluster of regions with similar GDP growth (x-axis) is the cause of no apparent linear relationship between GDP growth and the space-time lag of the percentage of urban population. In contrast, the second plot

(the right panel of Figure 15) is made based on the assumption that the change in the local percentage of the urban population (the *x*-axis) drives the change in the space-time lag of GDP growth (the *y*-axis). Due to the more varying percentage of urban population (*x*-axis), the linear pattern is shown better in the second scatter plot.

Figure 16

Scatter plot between GDP growth and the space-time lag of the percentage of urban population (left panel) and between the percentage of urban population and the space-time lag of GDP growth (right panel)
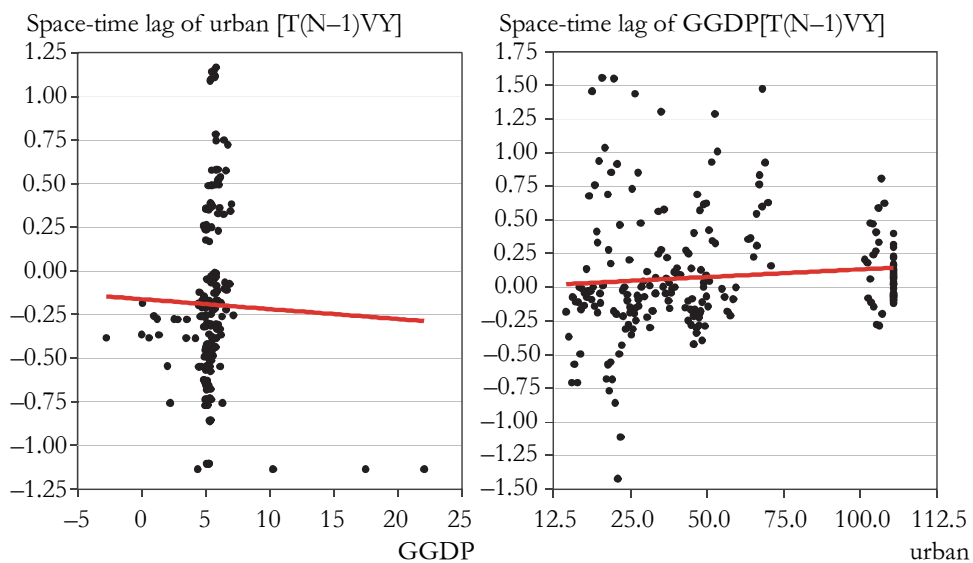
Even though the relationship can work in both directions, the information in table 5 and the patterns in Figure 16 give some insight regarding which variable acts as the cause of change. They indicate that the second type of relationship is more significant than the first one. Local urbanization is more likely to drive current and time lag neighbourhood GDP growth.

It has been discussed in the theoretical part that the index is used to measure the relationship degree and to identify the possible causal relationship between the local GDP growth vs. the space-time lag of the percentage of urban population or the local percentage of urban population vs. the space-time lag of GDP growth. If the focus is on identifying the influence of local urbanization on local GDP growth, then the setting of the space-time weight matrix must be changed by assuming no time and spatial dependence. In this way, the index becomes the weighted sum of Pearson-correlation for all *t*.

Concluding remarks

The key to accommodating the time dependence in the spatial cross-correlation measure for the spatial panel setting is the use of a modified spatial weight matrix in the space-time weight matrix. The simulation study confirms the good performance of the modified index in every possible degree of spatial and time dependence. A computational technique based on randomization is used to imitate the theoretical distribution of the proposed index for inference purposes. This approach is taken because it is data driven and more robust than the analytical approach under nonnormality.

Using the modified index, this study also confirms the significance of the time-dependent spatial cross-correlation between regional GDP growth and the percentage of the urban population of the 38 East Java regencies/municipalities (2014–2019). This result indicates that for the regions under study, it is more likely that urbanization drives the space-time lag of GDP growth. This interpretation of causality is made without employing several fallback measures (e.g., Granger Causality, IV analysis, Cointegration analysis). This study deals with short panel spatial data, in which employing fallback measures can be challenging. The spatial cross-correlation is indeed a relevant and appropriate measure in this case, especially where the relationship between variables highly depends on their spatial proximity. Time lags and natural sequencing are more suitable for time series data where the temporal order of events is more crucial.

Acknowledgement

REFERENCES

ABDEL-RAHMAN, A. N.–SAFARZADEH, M. R.–BOTTOMLEY, M. B. (2006): Economic growth and urbanization: A cross-section and time-series analysis of thirty-five developing countries: Rivista internazionale Di Scienze *Rivista Internazionale Di Scienze Economiche e Commerciali* 53 (3): 334–48.
https://doi.org/https://doi.org/10.1007/BF03029785

ANSELIN, L. (1995): Local indicators of spatial association – LISA *Geographical Analysis* 27 (2): 93–115. https://doi.org/10.1111/j.1538-4632.1995.tb00338.x

ANSELIN, L. (2001): Spatial econometrics. In: BALTAGI, B. H.: *A companion to theoretical econometrics* pp. 310–330. Blackwell Publishing Ltd.
https://doi.org/10.1002/9780470996249.ch15

ANSELIN, L.–LI, X.–KOSCHINSKY, J. (2022): GeoDa, from the desktop to an ecosystem for exploring spatial data *Geographical Analysis* 54 (3): 439–66.
https://doi.org/10.1111/gean.12311

ARIANOS, S.–CARBONE, A. (2009): Cross-correlation of long-range correlated series *Journal of Statistical Mechanics: Theory and Experiment* 2009 (03): P03037.
http://dx.doi.org/10.1088/1742-5468/2009/03/P03037

CHEN, M.–ZHANG, H.–LIU, W.–ZHANG, W. (2014): The global pattern of urbanization and economic growth: Evidence from the last three decades *PloS One* 9 (8): e103799.
https://doi.org/10.1371/journal.pone.0103799

CHEN, Y. (2013): New approaches for calculating Moran's index of spatial autocorrelation *PLoS ONE* 8 (7): e68336. https://doi.org/10.1371/journal.pone.0068336

CHEN, Y. (2015): A new methodology of spatial cross-correlation analysis *PLoS ONE* 10 (5): e0126158. https://doi.org/10.1371/journal.pone.0126158

CHENG, Y.–NING, C-L.–DU, W. (2020): Spatial cross-correlation models for absolute and relative spectral input energy parameters based on geostatistical tools *Bulletin of the Seismological Society of America* 110 (6): 2728–2742.
https://doi.org/10.1785/0120200142

DUFFY, G. P.–HUGHES-CLARKE, J. E. (2005): Application of spatial cross correlation to detection of migration of submarine Sand Dunes *Journal of Geophysical Research: Earth Surface* 110 (F4): S12. https://doi.org/10.1029/2004JF000192

DURAN, H. E.–KARAHASAN, B. C. (2022): Heterogenous responses to monetary policy regimes: A regional analysis for Turkey, 2009–2019 *Regional Statistics* 12 (3): 56–91.
https://doi.org/10.15196/RS120403

FITRIANI, R.–DARMANTO, D.–PUSDIKTASARI, Z. F. (2022): A dynamic-time dependent spatial autocorrelation detection for East Java's Covid-19 regional percent of cases, March 2020–March 2021 (Indonesia) *Regional Statistics* 12 (3): 18–53.
https://doi.org/10.15196/RS120302

FITRIANI, R.–PUSDIKTASARI, Z. F.–DIARTHO, H. C. (2020): The dynamic of 2011–2016 East Java's regional spatial growth, an exploratory spatial data Analysis *Journal of Economics and Business* 3 (2): 947–964.
http://dx.doi.org/10.31014/aior.1992.03.02.252

FITRIANI, R.–SUMARMININGSIH, E.–AMALIANA, L.–WIDHIASIH, N. D. (2023): The time-dependent spatial cross correlation, a study of East Java's regional GDP growth and percentage of urban, 2014–2019. In: *AIP Conference Proceedings*. Vol. 2903. AIP Publishing.

GOOD, P. (2013): *Permutation tests: A practical guide to resampling methods for testing hypotheses* Springer Science & Business Media, New York.
https://doi.org/10.1007/978-1-4757-2346-5

HENDERSON, V. (2003): The urbanization process and economic growth: The so-what question *Journal of Economic Growth* 8 (1): 47–71.
https://doi.org/10.1023/A:1022860800744

HONG, T.–YU, N.–MAO, Z.–ZHANG, S. (2021): Government-driven urbanisation and its impact on regional economic growth in China *Cities* 117: 103299.
https://doi.org/10.1016/j.cities.2021.103299

LAMB, A. P.–VAN WIJK, K.–LIBERTY, L. M.–MIKESELL, T. D. (2014): The spatial cross-correlation method for dispersive surface waves *Geophysical Journal International* 199 (1): 1–10. https://doi.org/10.1093/gji/ggu237

LIDDLE, B.–MESSINIS, B. (2013): *Which comes first – Urbanization or economic growth? Evidence from heterogeneous panel causality tests* University Library of Munich, Germany.

LOTH, C.–BAKER, J. W. (2013): A spatial cross-correlation model of spectral accelerations at multiple periods *Earthquake Engineering & Structural Dynamics* 42 (3): 397–417. https://doi.org/10.1002/eqe.2212

PESARIN, F.–SALMASO, L. (2010): The permutation testing approach: A review *Statistica* 70 (4): 481–509. http://dx.doi.org/10.6092/issn.1973-2201/3599

SCRUCCA, L. (2005): Clustering multivariate spatial data based on local measures of spatial autocorrelation *Quaderni Del Dipartimento Di Economia, Finanza e Statistica* 20 (1): 11.

SOLIHIN, A.–WARDANA, W. W.–FIDDIN, E.–SUKARTINI, N. M. (2021): Do government policies drive economic growth convergence? Evidence from East Java, Indonesia *Cogent Economics & Finance* 9 (1): 1992875. https://doi.org/10.1080/23322039.2021.1992875

WANG, Z.–LAM, N. S. N. (2020): Extending getis–Ord statistics to account for local space–Time autocorrelation in spatial panel data *The Professional Geographer* 72 (3): 411–420. https://doi.org/10.1080/00330124.2019.1709215

WHEELER, R. E.–TORCHIANO, M. (2010): Permutation tests for linear models in R *The Comprehensive R Archive Network* 1 (2): 1–36.

INTERNET SOURCES

ANSELIN, L. (2017): Global spatial autocorrelation *Bivariate, Differential and Eb Rate Moran Scatter Plot.* https://geodacenter.github.io/workbook/5b_global_adv/lab5b.html (downloaded: May 2023)

BPS-STATISTICS INDONESIA [BPS] (2021): *Produk domestik regional bruto kabupaten/kota provinsi Jawa Timur Menurut Lapangan Usaha 2016–2020.* Badan Pusat Statistik Provinsi Jawa Timur. www.bps.go.id (downloaded: May 2023)